Inorg. Chem. **2006**, *45*, 4359–4363

Structure of Anhydrous Alkali-Metal Formates

Michael P. Wilson, Nathaniel W. Alcock, and P. Mark Rodger*

Department of Chemistry, University of Warwick, Coventry CV4 7AL, U.K.

Received November 4, 2005

Single-crystal X-ray diffraction has yielded new crystal structures for cesium formate (CsOOCH) and rubidium formate (RbOOCH). The cesium formate structure has the same unit cell and space group as that published from powder X-ray diffraction data (Masuda, Y.; Yahata, A.; Ogawa, H. *Inorg. Chem.* **1995**, *34*, 3130–3133) but differs radically in the placement and orientation of the formate ions. The new crystal structure has been successfully modeled with an empirical force field based on pair potentials, whereas it proved impossible to develop a force field that gave an adequate description of the powder structure. For rubidium formate, the gross structure is similar to that previously published (Masuda, Y.; Morita, W.; Yahata, A.; Yukawa, Y. *Thermochim. Acta* **1998**, *318*, 39–43), but the space group includes a mirror plane (*Pbcm* rather than $Pbc2_1$). From this information, we have been able to analyze the effect of the cation size on the crystal structure for alkali-metal formates.

1. Introduction

Formates are common in nature, being a significant degradation product of biological material. NAD^+ reacts with formate to generate the energy required to drive biological processes.[1] Ionic forms of formates have been implicated in atmospheric aerosol nucleation.[2] They are being investigated as intermediates in the production of hydrogen for use as a clean fuel,[3] for which the cesium and rubidium formates have yielded the highest reaction rates. Cesium formate has found use in biology, as a dense liquid for fractionation of DNA samples,[4] while formate solutions have been shown to be effective precipitants for protein crystallography.[5,6] Alkali-metal formates have also been used as a selective hydrogen donor in palladium-catalyzed hydrogenation reactions[7,8] and shown to have considerable advantages as refrigerants[9] and deicers.[10] Most intriguingly, the spontaneous formation of microfibers has been reported, in which glassy fibers of $KHCO_3$ are filled with aqueous $KHCO_2$.[11]

Many of the experiments on alkali-metal formates have focused on the smaller cations, particularly sodium and potassium. This is probably largely due to their easy availability; however, developments in the petroleum industry over the past decade have brought cesium formate into the spotlight. Cesium formate (CsO_2CH) has become important in recent years as a major component of high-temperature, high-pressure drill-in and completion fluids for the petroleum industry.[12−15] Under these conditions, it has the advantages of stabilization of the polymer additives, compatibility with the formation waters, and stability in shale. Cesium formate is also biodegradable and gives an excellent drilling performance, yielding better than expected production rates with offshore wells. In some wells, however, conditions vary considerably between the well head and drilling point, with the oil passing through low-pressure, low-temperature zones in which there is a risk of crystallization. There is, therefore,

* To whom correspondence should be addressed. E-mail: p.m.rodger@warwick.ac.uk.

(1) Voet, D.; Voet, J. G.; Pratt, C. W. *Fundamentals of Biochemistry*; John Wiley & Sons Inc.: New York, 1999.
(2) Aloisio, S.; Hintze, P. E.; Vaida, V. *J. Phys. Chem. A* **2002**, *106*, 363−370.
(3) Onsager, O. T.; Brownrigg, M. S. A.; Lodeng, R. *Int. J. Hydrogen Energy* **1996**, *21*, 883−885.
(4) Rinehart, F. P.; Deininger, P. L.; Schmid, C. W. *Biochim. Biophys. Acta* **1978**, *520*, 21−37.
(5) McPherson, A. *Protein Sci.* **2001**, *10*, 418−422.
(6) Dunstone, M. A.; Kjer-Nielsen, L. B.; Kostenko, L.; Purcell, A. W.; Brooks, A. G.; Rossjohn, J.; McCluskey, J. *Acta Crystallogr. D* **2004**, *60*, 1425−1428.
(7) Baidossi, M.; Joshi, A. V.; Mukhopadhyay, S.; Sasson, Y. *Synth. Commun.* **2004**, *34*, 643−650.
(8) Basu, B.; Bhuiyan, M. M. H.; Jha, S. *Synth. Commun.* **2003**, *33*, 291−296.
(9) De Lucas, A.; Donate, M.; Molero, C.; Villasenor, J.; Rodriguez, J. F. *Int. J. Refrig.* **2004**, *27*, 324−330.
(10) Hellsten, P.; Nysten, T. *Water Sci. Technol.* **2003**, *48*, 45−50.
(11) Celio, H.; Lozano, J.; Cabibil, H.; Ballas, L.; White, J. M. *J. Am. Chem. Soc.* **2003**, *125*, 3302−3310.
(12) Hallman, J. H.; Vollmer, D. P. *Hart's Pet. Eng. Int.* **1998**, *71*, 83−89.
(13) Anonymous. *Chem. Mark. Rep.* **1998**, *253*, 15.
(14) Hands, N.; Kowbel, K.; Maikranz, S.; Nouris, R. *Oil Gas J.* **1998**, *96*, 65−69.
(15) Dobson, J. W.; Cashion, J. P.; Bellew, B. B. U.S. Patent 5,804,535, 1998.

10.1021/ic051910q CCC: $33.50
Published on Web 05/03/2006

Table 1. Crystal Data for Cesium and Rubidium Formates, Obtained from Single-Crystal Studies (This Work) and the Data of Masuda and Co-workers[16,17]

	cesium formate (single)	cesium formate (powder; Masuda et al., 1995)	rubidium formate (single)	rubidium formate (single; Masuda et al., 1998)[a]
chemical formula	$CsCHO_2$	$CsCHO_2$	$RbCHO_2$	$RbCHO_2$
fw	178.00	178.00	130.49	130.49
cryst syst	orthorhombic	orthorhombic	orthorhombic	orthorhombic
space group	*Pbcm*	*Pbcm*	*Pbcm*	$Pbc2_1$
Z	4	8	4	4
a (Å)	4.7938(3)	4.785(1)	4.6172	4.630(2)
b (Å)	9.5339(6)	9.553(2)	9.1822	9.229(1)
c (Å)	7.9101(5)	15.927(2)	7.3525	7.408(2)
T (K)	180(2)	[room temp?]	180(2)	[room temp?]
cryst color, form	colorless, blocks		colorless, blocks	
cryst size (mm)	0.40 × 0.40 × 0.40		0.40 × 0.22 × 0.20	0.5 × 0.4 × 0.3
μ (mm^{-1})	10.02		15.63	15.63
T_{min}, T_{max}	0.34, 0.83		0.44; 0.89	0.86, 1.00
reflns: measd, independent, obsd [$I > 2\sigma(I)$]	2138, 1006, 644		849, 257, 196	591, (591?), 323 [$I > 3\sigma(I)$]
R_{int}	0.057		0.046	
θ_{max} (deg)	25.9		28.5	35
R [$F^2 > 2\sigma(F^2)$], wR (F^2), S	0.036, 0.084, 0.88		0.074, 0.179, 1.01	0.086, 0.110
no. of param	25		25	22
weighting scheme (a)[b]	0.0600		0.15	
δF_{max}, δF_{min} (e $Å^{-3}$)	1.83, −1.75		3.15, −2.28	
extinction coeff	0.025(2)		0.12(3)	

[a] a and b exchanged compared to the published data, to match our cell setting. [b] $w = 1/[\sigma^2F_o^2) + (aP)^2]$, where $P = (F_o^2 + 2F_c^2)/3$.

a need to develop efficient chemical additives for controlling the crystallization of cesium formate.

In an attempt to design such additives, the authors have initiated a molecular modeling study of cesium formate. As a first step toward this goal, attempts were made to derive empirical force fields that reproduced the powder X-ray diffraction (XRD) structure for cesium formate.[16] However, this process proved to be problematic. No combination of van der Waals, electrostatic, polarizable, and intramolecular (stretch, angle, improper torsion, etc.) bond interactions was found that would generate a stable structure in agreement with the powder XRD. Inspection of the powder structure showed that it contains intermolecular O−O distances of 2.7 Å, which is implausibly small in the absence of hydrogen bonding and when the atoms in question do not complex the same metal center.

In this paper, we report single-crystal determinations of the low-temperature anhydrous structure for both cesium and rubidium formates. For the cesium salt, the new structure differs radically from that reported from powder XRD studies.[16] The closest nonbonded O−O distance is now 3.581(6) Å, which is consistent with distances observed for all other alkali-metal formates, and the new structure was found to be amenable to analysis with molecular force fields. The gross structure for rubidium formate is unchanged from the previous structure,[17] but a higher symmetry space group is indicated. The studies reported here complete the series of single-crystal structures for anhydrous alkali-metal formates from sodium to cesium and have thus permitted us to examine the trends in structure as the cation is varied down the periodic table.

2. Experimental Section

Analytical-reagent standard cesium or rubidium formate from Aldrich Chemical Co. was dissolved in a minimum of methanol in polypropylene containers. After filtration of the solution, the open container was placed inside a large polypropylene container containing a small amount of either 1-butanol or tetrahydrofuran (THF) and the whole system sealed immediately. Crystallization was continued, with occasional swirling of the suspension, over a 2-week period, after which the crystals were collected. For the cesium salt, the best crystals were those grown with THF, while with rubidium, butanol gave better crystals. For both salts, the crystals are extremely hygroscopic and difficult to handle, but a single crystal of cesium formate with only minor satellites was eventually identified. For neither crystal were faces visible to carry out analytical absorption corrections, so only the SADABS multiscan procedure was possible.

The crystal data and refinement details are given in Table 1. A Siemens *SMART*[18] three-circle system with a CCD area detector was used. The crystals were held at 180(2) K with the Oxford Cryosystem Cryostream Cooler.[19] No phase transitions were observed in the temperature range 283−180 K. For the cesium salt, systematic absences indicated either space group *Pbcm* or $Pbc2_1$ (nonstandard setting of $Pca2_1$). The structure was initially examined using the large cell (c-doubled) found by Masuda et al.,[16] in space group $P1$. The cesium atoms were located from a Patterson synthesis and the light atoms then found by Fourier syntheses. The center of inversion was then located, and it was found that the halved-c cell could be used without any significant unexplained intensity (only 14 of 1979 reflections having any intensity greater than the 3σ level). After refinement, the presence of additional symmetry corresponding to space group *Pbcm* was identified and the refinement completed in this space group. The hydrogen atom was added at its calculated position and refined using a riding model. Anisotropic displacement parameters were used for all non-

(16) Masuda, Y.; Yahata, A.; Ogawa, H. *Inorg. Chem.* **1995**, *34*, 3130−3133.
(17) Masuda, Y.; Morita, W.; Yahata, A.; Yukawa, Y. *Thermochim. Acta* **1998**, *318*, 39−43.
(18) Siemens. *SMART User's Manual*; Siemens Industrial Automation Inc.: Madison, WI, 1994.
(19) Cosier, J.; Glazer, A. M. *J. Appl. Crystallogr.* **1986**, *19*, 105−107.

Table 2. Atomic Coordinates (x, y, z) for Cesium and Rubidium Formates, Obtained from Single-Crystal Studies[a]

		cesium formate	rubidium formate
origin		1	1
Cs or Rb	x	0.04647(10)	0.05845(19)
	y	0.2500	0.2500
	z	0.0000	0.0000
C	x	0.5998(15)	0.6100(20)
	y	0.0446(6)	0.0481(13)
	z	0.7500	0.7500
H	x	0.45249	0.45460
	y	−0.02200	−0.01990
	z	0.7500	0.7500
O(1)	x	0.5313(10)	0.5450(15)
	y	0.1724(4)	0.1790(9)
	z	0.7500	0.7500
O(2)	x	0.8442(10)	0.8643(16)
	y	−0.0029(4)	−0.0034(8)
	z	0.7500	0.7500

[a] A comparison with the coordinates published from powder XRD studies is given in the Supporting Information, Table S1.

hydrogen atoms; the hydrogen atom was given an isotropic displacement parameter equal to 1.2 times the equivalent isotropic displacement parameter of the atom to which it is attached. The largest difference peaks and holes are all close to cesium atom positions.

For rubidium formate, the best crystal found still showed substantial multiple components, and only the first frame set could be satisfactorily integrated. Systematic absences indicated either space group *Pbcm* or $Pbc2_1$ (nonstandard setting of $Pca2_1$). The former was chosen by analogy with cesium formate and shown to be correct by successful refinement. The structure was solved by substitution of the coordinates of cesium formate. The determination by Masuda et al.[17] only became known to us at this stage. Their and our structures are essentially the same, apart from their choice of the noncentrosymmetric space group $Pbc2_1$ rather than *Pbcm*, for which no rationale was presented. Refinement of our data in the lower-symmetry space group was attempted, but this produced no improvement in the R value, and we see no reason for choosing it rather than the centrosymmetric alternative. The relatively large maximum difference Fourier peak and hole are located close to the rubidium atom and are attributed to twin and absorption effects.

For both structures, Table 1 provides crystal data and Table 2 the coordinates, both compared to the previous results.

3. Results and Discussion

3.1. Crystal Structures of Rubidium and Cesium Formates. The crystal structures of cesium and rubidium formates as determined from single-crystal XRD were found to be isomorphous, and so cesium formate will be used here as the focus for a detailed description. Low-temperature cesium formate crystallizes in orthorhombic space group 57 with unit cell dimensions of 4.7938, 9.5339, and 7.9101 Å (Figure 1). The cesium ions are at the vertexes of an array of slightly distorted tetragonal cells, each of which contains a formate ion near its center. The formate ions are oriented parallel to the $a-b$ plane. The net effect is that the crystal structure consists of planar arrays of formate ions alternating with planes of Cs^+ ions normal to the crystallographic c axis. Within each formate plane, the orientation of the formate ions alternates so that the C−H bond direction makes an angle of +42° and then −42° to the b vector. Along the c direction, alternate formate ions are stacked with an anti-parallel arrangement.

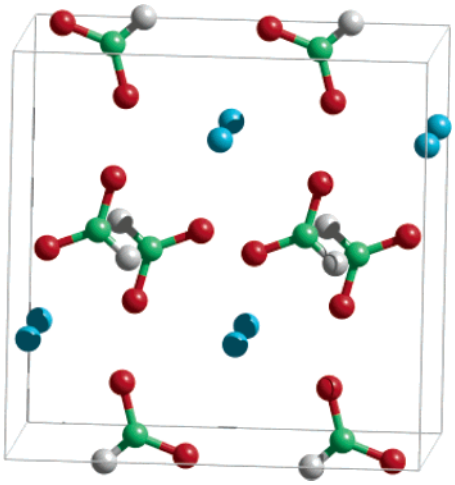

Figure 1. 2 × 1 × 1 unit cell of cesium formate from the single-crystal XRD analysis (this work). Color key: Cs, blue; C, green; O, red; H, gray.

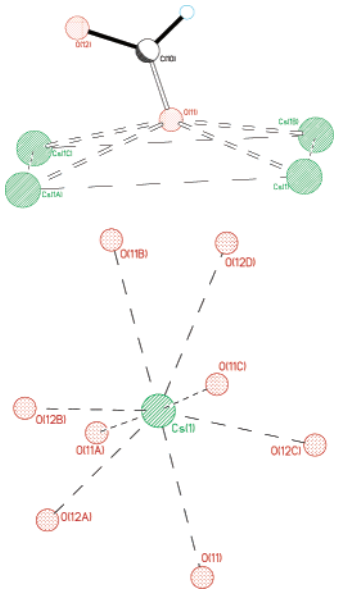

Figure 2. Environment of the oxygen atoms and the Cs ion. Color key: O, red; Cs, green; C, black; H, light blue.

The local environment of both the formate oxygen and cesium atoms is illustrated in Figure 2. Each C−O bond points to the center of a rectangular face of the cesium sublattice, with the oxygen atom being nearly coplanar with its four nearest cesium ions. Although each Cs^+ has eight neighbor formate ions, two of these are much further away (4.63 Å compared with 3.51−3.84 Å) and have the hydrogen atom oriented toward the Cs^+ ion. Thus, it would be more appropriate to describe each Cs^+ ion as having just six formate ions in its coordination shell. Two of these formates present both oxygen atoms to the Cs^+ ion in a symmetric pattern, so that the cation is coordinated by eight oxygen atoms (Figure 2).

The single-crystal structure reported here (Figure 1 and Table 2) differs from the powder XRD structure (Supporting Information, Figure S1 and Table S1) primarily in the location of the formate ions: the new coordinates place the

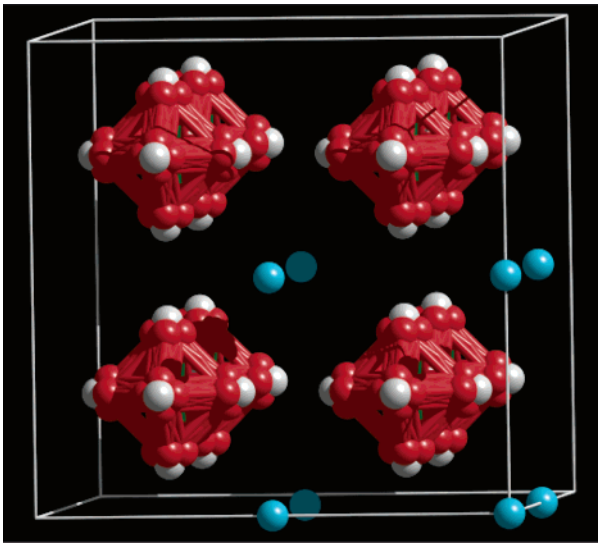

Figure 3. 2 × 2 × 2 unit cells of the cesium formate cubic phase, which forms above 36 °C. The diagram shows the orientational degeneracy of the formate ion.

Table 3. Shortest Intermolecular Atom−Atom Distances for Cesium and Rubidium Formates

	d (Å)	
atoms	$CsHCO_2$	$RbHCO_2$
O−O	3.58	3.48
O−H	2.91	2.73
$O-M^+$	3.120(3)	2.94
O−C	3.60(1)	3.46
C−C	4.16(1)	3.91
H−C	3.97	3.70
H−H	4.00	3.72
M^+-C	3.510(3)	3.33
M^+-H	3.79	3.59
M^+-M^+	3.96	3.68

formate in the middle of eight cesium ions (compared with four for the powder XRD structure). Differences are also apparent in the orientation of the formate ions. In the new structure, the formate ions lie completely within the *a*−*b* plane, instead of twisted about the *a* axis as in the powder XRD structure. As will be discussed below, this new arrangement is more consistent with the trend observed in sodium, potassium, and rubidium formates. The new, single-crystal, structure also gives a much more intuitive understanding of the phase transition to the cubic phase, observed[16] to occur at 36 °C (see Figure 3) than that which arises from the earlier structure: increasing the temperature simply leads to rotational disordering of the formate orientations, resulting in a pseudooctahedral symmetry for the anion and allowing the cesium sublattice to adopt cubic symmetry.

Nearest-neighbor interatomic distances are listed in Table 3. It can be seen that the present results avoid the implausibly short intermolecular O−O distances of the published powder XRD structure (Supporting Information, Table S2). The shortest O−O distance is now found to be 3.581(6) Å, which is typical of the other anhydrous alkali-metal formates (see section 4). Eight oxygen atoms surround each Cs^+ ion, and four cesium ions surround each oxygen atom. Two of these cesium ions coordinate both oxygen atoms within the same formate molecular ion, so that the formate ion is surrounded by six nearest-neighbor cesium ions.

For the rubidium formate structure, the differences between the new single-crystal and published powder XRD structures are not as great as those for cesium formate. We do find a higher-symmetry structure (space group *Pbcm*), leading to a completely planar arrangement of the formate ions. The nearest-neighbor distances in the new rubidium formate structure are similar to those for the new cesium structure (Table 3), with just the decrease expected for substitution of cesium by the smaller rubidium ion.

3.2. Molecular Modeling of the Crystalline Alkali-Metal Formates. Because no force field for cesium formate has been reported in the literature, the cesium formate structure reported here was used with the GULP program[20] to derive an empirical force field. An acceptable fit was possible using just van der Waals and electrostatic intermolecular interactions. It is worth noting that, even with the inclusion of polarization effects, no adequate potential could be fitted to the powder XRD structure.[16]

The fitted potential and corresponding minimum-energy structure is reported in the Supporting Information (Tables S3 and S4); the energy optimization was performed without any symmetry constraints. No major differences from the experimental structure are found in either the unit cell lengths or atomic coordinates within the unit cell. The special position atomic coordinates (e.g., at 0.2500, 0.5000, and 0.7500) are reproduced exactly even in the absence of any symmetry constraints. The mean of the deviation from the single-crystal data for atomic positions is 0.0046 Å with a standard deviation of 0.0123 Å. For the unit cell vectors, the absolute mean deviation is 0.0642 Å with a standard deviation of 0.0623 Å. A graphical overlay of the predicted and measured structures (Supporting Information, Figure S2) confirms the closeness of this fit. These results indicate that the current force field accurately models the calculated structure. More detailed modeling studies with this potential will be reported elsewhere.[21]

4. Trends in the Anhydrous Alkali-Metal Formate Crystal Structures

The newly determined single-crystal structures of rubidium and cesium formates now complete the anhydrous series from Na to Cs and allow one to analyze the role of the cation in determining the low-temperature crystal structures of the alkali-metal formates; only the hydrated lithium formate structure is available,[22] so this is not further considered.

In general, all of the structures can be understood in terms of planar arrays of formate anions, moderated by the packing constraints induced by different cation sizes. For K^+ and bigger cations, the formate ions lie entirely within planes parallel to the *a*−*b* plane and alternate with planes of M^+ ions. The M^+ sublattice is nearly tetragonal and arranged

(20) Gale, J. D. *J. Chem. Soc., Faraday Trans.* **1997**, *93*, 629−637.
(21) Wilson, M. P.; Panchmatia, P.; Rodger, P. M., manuscript in preparation.
(22) Thomas, J. O.; Tellgren, R.; Almlof, J. *Acta Crystallogr. B* **1975**, *31*, 1946.

Table 4. Geometry of Formate Planes and the M^+−Formate Coordination Shell[a]

			d_{OO} (Å)		M^+−formate environment				
cation	angle: C−H and *b*	formate tilt	intraplane	interplane	no. of equivalent HCO_2^- pairs	C−M−C angle	d_{MC} (Å)	nearest atom	d_{MO} (Å)
Na	0	39	3.59	3.21	1	180	2.80	O, O	2.59
							3.95	H	
					1	159.6	3.17	O	2.39
							3.17	O	2.39
					1	145.9	3.19	O	2.42
							3.19	O	2.42
K	0	0	3.47	3.71	1	180	3.24	O, O	3.00
							3.24	O, O	3.00
					2	180	3.49	O	2.82
							3.49	O	2.82
					1	180	4.43	H	
							4.43	H	
Rb	±41	0	3.48	3.88	2	173.9	3.33	O, O	3.07, 3.10
							3.65	O	2.97
					2	161.1	3.64	O	2.94
							4.52	H	
Cs	±42	0	3.58	4.22	2	180	3.51	O, O	3.25, 3.26
							3.84	O	3.14
					2	164.2	3.83	O	3.12
							4.63	H	

[a]Formate ions in the coordination shell have been grouped into pairs of formate ions on opposite sides of the M^+ ion.

such that eight cations surround each anion. The Na^+ ion is sufficiently small that it fits within interstices in the formate layers, thus giving rise to planar arrays of Na^+HCOO^- ion pairs. In the process, the interlayer distance becomes so small that the formate ions twist so that the oxygen atoms move out of the formate planes, giving corrugated planes that can better accommodate the short interplanar O−O distances (3.21 Å; Table 4).

Most intriguingly, there is remarkable consistency in the closest intermolecular O···O distances. All four structures give closest in-plane O···O contacts close to 3.5 Å (Table 4), despite the fact that there are three quite different orientational patterns for the formate planes within these four structures. One explanation for this is that the structure of the formate layers is dominated by efficient packing of polar oxygen atoms. However, the propensity to maintain O···O contacts within a planar array, despite the large partial negative charges on these atoms, is also suggestive of some intermolecular delocalization of the formate π electrons. Either way, it is clear that formate−formate interactions play a substantive role in determining the crystal structure.

A common feature of all four structures is the formation of bifurcated $M^+\cdots{}^-O_2CH$ pairings. Each formate binds to just one Na^+ ion in this way, resulting in an ion pair. For K^+, Rb^+, and Cs^+ ions, each formate ion couples to two cations through both oxygen atoms: one above the plane of the formate molecule and one below it. Each cation also participates in two bifurcated interactions, leading to infinite chains of such ion pairings. It is interesting to note that bifurcated interaction does not lead to the shortest $O\cdots M^+$ distances: in every case, the oxygen from a singly coordinating formate is 0.1−0.2 Å closer than that from the doubly coordinating anion, with the greatest difference occurring with the smallest cation (Table 4). This indicates that simple electrostatic interaction cannot be dominating the nearest-neighbor cation−anion interactions.

5. Conclusions

In this paper, we have presented single-crystal determinations of the structures of anhydrous rubidium and cesium formates. The structures reported here differ from the previously reported structures and remove the main anomalies observed in that of cesium formate. The new structures complete the series of anhydrous alkali-metal formates from sodium to cesium and so have allowed us to analyze the structural trends down the group I elements (excluding lithium, for which no anhydrous structure is presently available). All of the structures are based on planar arrays of formate molecular ions, and all show essentially the same shortest intermolecular O···O distance within these planes. This may be indicative of interesting electronic coupling between the formate molecules.

Each of the alkali-metal formate crystal structures shows evidence of the cation interacting with both oxygen atoms from a given formate ion (a bifurcated interaction). Although these bifurcated interactions give the shortest M^+−formate distances, it is singly-donating formate ions that generate the shortest M^+−O distances. The number of such bifurcated interactions is consistent with variations in the cation size, but their location about the cation suggests that favorable formate−formate interactions compete with anion−cation electrostatics to determine the arrangement of formates within the crystal structure.

Acknowledgment. This work was supported by Cabot Specialty Fluids Inc.

Supporting Information Available: X-ray crystallographic data (CIF), tables of atomic coordinates, shortest intermolecular atom−atom distances, intermolecular potentials, and a comparison of the single-crystal and calculated structures of cesium formate, and figures of a 2 × 1 × 1 unit cell and a comparison of the single-crystal and calculated structures of cesium formate. This material is available free of charge via the Internet at http://pubs.acs.org.

IC051910Q